UNLV | University Libraries
University of Nevada, Las Vegas

Environmental Studies Faculty Publications | Harry Reid Center for Environmental Studies

12-2001

Large Nondipole Effects in the Angular Distributions of K-Shell Photoelectrons from Molecular Nitrogen

Oliver Hemmers
University of Nevada, Las Vegas, Oliver.Hemmers@unlv.edu

H. Wang
Lund University

P. Focke
University of Tennessee, Knoxville

I. A. Sellin
University of Tennessee - Knoxville

Dennis W. Lindle
University of Nevada, Las Vegas, lindle@unlv.nevada.edu
Follow this and additional works at: https://digitalscholarship.unlv.edu/hrc_fac_articles

 Part of the Atomic, Molecular and Optical Physics Commons, Inorganic Chemistry Commons, Nuclear Commons, and the Physical Chemistry Commons
See next page for additional authors

Repository Citation

Hemmers, O., Wang, H., Focke, P., Sellin, I. A., Lindle, D. W., Arce, J. C., Sheehy, J. A., Langhoff, P. W. (2001). Large Nondipole Effects in the Angular Distributions of K-Shell Photoelectrons from Molecular Nitrogen. *Physical review letters, 87*(27), 273003-1-273003-4.
https://digitalscholarship.unlv.edu/hrc_fac_articles/26

This Article is protected by copyright and/or related rights. It has been brought to you by Digital Scholarship@UNLV with permission from the rights-holder(s). You are free to use this Article in any way that is permitted by the copyright and related rights legislation that applies to your use. For other uses you need to obtain permission from the rights-holder(s) directly, unless additional rights are indicated by a Creative Commons license in the record and/or on the work itself.

This Article has been accepted for inclusion in Environmental Studies Faculty Publications by an authorized administrator of Digital Scholarship@UNLV. For more information, please contact digitalscholarship@unlv.edu.

Authors

Oliver Hemmers, H. Wang, P. Focke, I. A. Sellin, Dennis W. Lindle, J. C. Arce, J. A. Sheehy, and P. W. Langhoff

This article is available at Digital Scholarship@UNLV: https://digitalscholarship.unlv.edu/hrc_fac_articles/26

Large Nondipole Effects in the Angular Distributions of K-Shell Photoelectrons from Molecular Nitrogen

O. Hemmers,[1] H. Wang,[1,2] P. Focke,[3,4] I. A. Sellin,[3] and D. W. Lindle[1]

[1]*Department of Chemistry, University of Nevada, Las Vegas, Nevada 89154-4003*
[2]*MAX-Lab, Lund University, Box 118, 22100 Lund, Sweden*
[3]*Department of Physics, University of Tennessee, Knoxville, Tennessee 37996*
[4]*Centro Atomico Bariloche, RA-8400 Bariloche, Argentina*

J. C. Arce,[5] J. A. Sheehy,[6] and P. W. Langhoff[6,7,8]

[5]*Departamento de Quimica, Universidad del Valle, A.A. 25360 Cali, Colombia*
[6]*Air Force Research Laboratory, AFRL/PRS, Edwards AFB, California 93524-7680*
[7]*Department of Chemistry, Indiana University, Bloomington, Indiana 47405*
[8]*San Diego Supercomputer Center, University of California, 9500 Gilman Drive, La Jolla, California 92093-0505*

(Received 20 February 2001; revised manuscript received 25 October 2001; published 13 December 2001)

Measurements of angular distributions of K-shell electrons photoejected from molecular nitrogen are reported which reveal large deviations at relatively low photon energies ($\hbar\omega \leq 500$ eV) from emission patterns anticipated from the dipole approximation to interactions between radiation and matter. A concomitant theoretical analysis incorporating the effects of electromagnetic retardation attributes the observed large nondipole behaviors in N_2 to bond-length-dependent terms in the $E1 \otimes (E2, M1)$ photoelectron emission amplitudes which are indicative of a potentially universal nondipole behavior in molecular photoionization.

DOI: 10.1103/PhysRevLett.87.273003 PACS numbers: 33.60.Fy, 33.80.Eh

The electric-dipole or uniform-electric-field approximation has long served as a basis for understanding many aspects of the interactions between radiation and matter [1,2]. In this limit, the angular distributions of electrons photoejected from atoms and molecules by linearly polarized radiation are described by the expression

$$d\sigma(\hat{\boldsymbol{k}}_e; \hbar\omega)/d\Omega_{\hat{\boldsymbol{k}}_e} = \{\sigma(\hbar\omega)/4\pi\} \times \{1 + \beta(\hbar\omega)P_2(\cos\theta_e)\}, \quad (1)$$

where $\hat{\boldsymbol{k}}_e = \phi_e, \theta_e$ is the laboratory-frame direction of the ejected electron, $\sigma(\hbar\omega)$ is the partial photoionization cross section for production of a specific ionic state, $P_2(\cos\theta_e)$ is the second Legendre polynomial in the polar ejection angle relative to the photon polarization vector, and $\beta(\hbar\omega)$ is the dipole anisotropy factor [1–4].

Deviations from Eq. (1) for atomic targets can be attributed to the variation in phase of the incident radiation over the spatial dimensions of the absorbing charge distributions [5], treatments of which require incorporation of additional (electric quadrupole, magnetic dipole, ...) terms in the radiation-matter interaction [6–8]. Accordingly, significant departures from Eq. (1) are commonly thought to occur only at wavelengths comparable with or smaller than the spatial dimensions of the absorbing electronic shells, an expectation confirmed by recent experimental photoionization studies on rare-gas atoms performed at sufficiently high photon energies [9,10]. Surprisingly, however, atoms have been shown recently to exhibit nondipole effects in photoelectron angular distributions beyond the predictions of Eq. (1) even at longer incident wavelengths [11–14].

The present Letter reports experimental observations and corresponding theoretical studies of significant deviations from Eq. (1) in the angular distributions of K-shell electrons emitted from gas-phase N_2 molecules. These deviations are found at surprisingly low ($\hbar\omega \leq 500$ eV) incident photon energies in N_2, and they exhibit resonance-like variation with photon energy in the relevant nondipole anisotropy factor. A detailed theoretical analysis of the contributions of (electric-quadrupole, magnetic-dipole) terms first order in photon momentum for interactions between radiation and matter attributes the observed behavior to the presence of bond-length-dependent $E1 \otimes (E2, M1)$ photoionization amplitudes and suggests that the present results in N_2 may be indicative of a universal behavior in molecular photoionization.

The measurements were performed at the Advanced Light Source (ALS) at the Lawrence Berkeley National Laboratory on undulator beam line 8.0, which provides nearly 100% linearly polarized photons in the 100 to 1300 eV energy range. The ALS, operated in the two-bunch mode, provides a photon pulse every 328 ns, allowing photoelectron detection using a time-of-flight (TOF) spectrometer described in detail elsewhere [15]. This apparatus can rotate around the photon-beam axis and employs four simultaneously recording electron-energy analyzers at different angles to detect Auger and photoelectrons. Two of the analyzers are located in the "dipole" plane perpendicular to the direction of photon propagation and are separated by a fixed angle of 125.3°. The other two ("nondipole") analyzers are positioned at 12 and 3 o'clock on a cone of 35.3° half angle whose axis is along the

 © 2001 The American Physical Society

photon-beam direction. Spectra of air and of air/xenon mixtures were taken for ≈600 sec each, providing the N_2 $1s$ photoelectron features, as well as known Auger lines for electron-energy and relative analyzer-transmission calibration. The N_2 $1s$ data also were calibrated for analyzer transmission using Ne $1s$ and Ar $2p$ photoemission, in which cases accurate calculations have been performed [16]. All of the calibration methods yielded consistent results for the N_2 $1s$ dipole and nondipole angular-distribution measurements.

Nondipole effects in photoionization are detected by orienting the TOF analyzers in accordance with the angular distributions expected when contributions first order in photon momentum ($\hbar k_p$) are included in the development. In this case, the differential cross section of Eq. (1) is modified to take the more general form [5–14]

$$d\sigma(\hat{\boldsymbol{k}}_e;\hbar\omega)/d\Omega_{\hat{\boldsymbol{k}}_e} = \{\sigma(\hbar\omega)/4\pi\}\{1 + \beta(\hbar\omega)P_2(\cos\theta_e) + [\delta(\hbar\omega) + \gamma(\hbar\omega)\cos^2\theta_e]\sin\theta_e\cos\phi_e\}, \quad (2)$$

where $\sigma(\hbar\omega)$ and $\beta(\hbar\omega)$ are the dipole parameters of Eq. (1), $\delta(\hbar\omega)$ and $\gamma(\hbar\omega)$ are the first-order nondipole anisotropy parameters, the photon polarization direction defines the z axis employed, and $\boldsymbol{k}_p$ is along the positive x axis. Referring to Eq. (2), one of the dipole analyzers is set at the dipole "magic" polar angle $\theta_e = \theta_m \approx 54.7°$, with $\phi_e = 90°$, in which case $P_2(\cos\theta_m) = 0$ and Eq. (2) reduces to $(d\sigma/d\omega)_1 = \sigma(\hbar\omega)/4\pi$. The nondipole analyzer at 3 o'clock is positioned similarly except $\phi_e = 0°$, in which case Eq. (2) becomes $(d\sigma/d\omega)_2 = [\sigma(\hbar\omega)/4\pi][1 + (2/27)^{1/2}][3\delta(\hbar\omega) + \gamma(\hbar\omega)]$ for this detector. The ratio $(d\sigma/d\omega)_2/(d\sigma/d\omega)_1 = [1 + (2/27)^{1/2}] \times [3\delta(\hbar\omega) + \gamma(\hbar\omega)]$ provides the indicated combination $\zeta(\hbar\omega) \equiv 3\delta(\hbar\omega) + \gamma(\hbar\omega)$ of nondipole parameters when the spectra are suitably normalized for relative transmission. The other two analyzers provide information for determining values of $\beta(\hbar\omega)$ and for establishing consistency of the $\zeta(\hbar\omega)$ measurements.

Employing the foregoing approach, spectra from the dipole and nondipole magic-angle analyzers taken simultaneously at the same incident photon energy can be consistently normalized using known Auger and photoemission lines, providing the nondipole parameter $\zeta(\hbar\omega)$ at this energy from the aforementioned ratio. Note in this connection that the angular distributions of Auger electrons are given to first order in the photon momentum by the distribution of Eq. (1), where $\sigma(\hbar\omega)$ and $\beta(\hbar\omega)$ refer to appropriate Auger values in this case; that is, nondipole effects on Auger-electron angular distributions for good parity targets contribute only in second order in the photon momentum [17–19]. Accordingly, because both the dipole and nondipole analyzers are set at the magic polar angle, Auger-electron intensities detected by the two analyzers can be expected to be identical up to terms second order in photon momentum.

In Fig. 1 are shown $\zeta(\hbar\omega)$ values for N_2 obtained as indicated above. The inset in the figure depicts typical dipole and nondipole Auger and photoelectron spectra taken at 500 eV photon energy normalized using the N_2 KLL (K-shell hole, L-shell electrons) Auger lines present in both spectra. The broad peak centered at ≈470 eV photon energy in the measured nondipole anisotropy factor is due to significant contributions from the nondipole terms in Eq. (2) to the angular distributions of molecular photoelectrons having a broad range of kinetic energies. Additionally, the data show evidence of a possible oscillation at higher photon energies, behavior not present in previously reported atomic nondipole anisotropy measurements [9–14].

The origins of the resonancelike photon-energy variations in Fig. 1 ultimately depend upon the phase variation of the incident radiation over the target molecule and its consequent effect on the photoionization matrix elements, differential in ejection angle, describing the ionization process [1,2]. Based on this general formalism, a recent theoretical development [20] specifically appropriate for molecules provides explicit expressions for the nondipole $E1 \otimes (E2, M1)$ parameters first order in photon momentum appearing in Eq. (2). For diatomic molecules, this

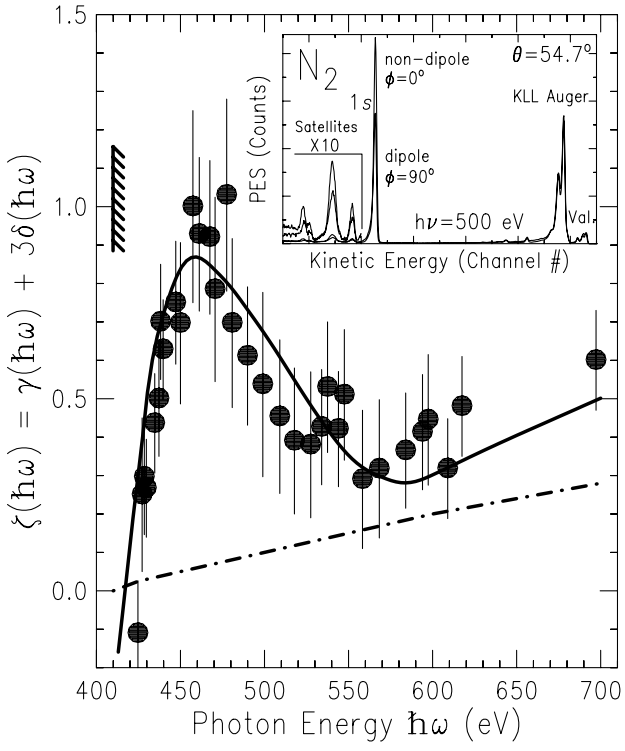

FIG. 1. Nondipole anisotropy parameter $\zeta(\hbar\omega) \equiv 3\delta(\hbar\omega) + \gamma(\hbar\omega)$ for K-shell photoemission from molecular nitrogen: the solid circles and the solid curve refer to experimental and theoretical values as described in the text, respectively; the dash-dotted curve gives the atomic limit obtained employing Eq. (5). The inset shows dipole and nondipole TOF-electron spectra used to determine experimental values of $\zeta(\hbar\omega)$ as described in the text.

development yields expressions [Eqs. (23) and (24) of Ref. [20]] for $\delta(\hbar\omega)$ and $\gamma(\hbar\omega)$ in terms of *body-frame* dipole and nondipole transition moments and angular emission amplitudes. Combining these results gives the expression

$$\zeta(\hbar\omega) \equiv \gamma(\hbar\omega) + 3\delta(\hbar\omega) = \frac{1}{\sigma(\hbar\omega)} \sum_{\lambda_D,\lambda_Q} \sum_{\lambda_1,\lambda_3} \mu_D^{(\lambda_D)} \mu_Q^{(\lambda_Q)} 2\,\mathrm{Re}\{\langle \hat{\Theta}_D^{(\lambda_D)} | a_{\lambda_D,\lambda_Q}^{(\lambda_1)} P_1^{(\lambda_1)} + b_{\lambda_D,\lambda_Q}^{(\lambda_3)} P_3^{(\lambda_3)} | \hat{\Theta}_Q^{(\lambda_Q)} \rangle\}, \quad (3)$$

where $\sigma(\hbar\omega)$ is the partial cross section appearing in Eq. (2), $\mu_D^{(\lambda_D)}$ and $\hat{\Theta}_D^{(\lambda_D)}(\theta_b)$ ($\lambda_D = 0, \pm 1$) are body-frame dipole transition moments and angular emission amplitudes, respectively, $\mu_Q^{(\lambda_Q)}$ and $\hat{\Theta}_Q^{(\lambda_Q)}(\theta_b)$ ($\lambda_Q = 0, \pm 1, \pm 2$) are corresponding nondipole quantities, $P_1^{(\lambda_1)}(\theta_b)$ and $P_3^{(\lambda_3)}(\theta_b)$ refer to normalized associated Legendre functions in the body-frame polar angle [21], the integral is over the angle θ_b only, $\mathrm{Re}\{\cdots\}$ refers to the real part of the enclosed quantity, and $a_{\lambda_D,\lambda_Q}^{(\lambda_1)}$ and $b_{\lambda_D,\lambda_Q}^{(\lambda_3)}$ are previously reported constants [20].

Application of Eq. (3) to the degenerate K shells $(1\sigma_g^2, 1\sigma_u^2)$ of molecular N_2 entails evaluation of four separate dipole $(1\sigma_{g/u} \rightarrow k\sigma_{u/g}, k\pi_{u/g})$ continuum transition moments and corresponding angular emission amplitudes and six separate nondipole $(1\sigma_{g/u} \rightarrow k\sigma_{g/u}, k\pi_{g/u}, k\delta_{g/u})$ moments and amplitudes, as well as 26 individual angular integrals involving the associated Legendre polynomials. In view of this relative complexity, it is helpful to first consider the high-photon-energy limit of the expressions for $\delta(\hbar\omega)$ and $\gamma(\hbar\omega)$, where the effects of photoelectron rescattering by the molecular field are neglected. The angular emission amplitudes for dipole and nondipole photoionization in this limit are [20]

$$\hat{\Theta}_D^{(\lambda_D)}(\theta_b) \rightarrow -iP_1^{(\lambda_1)}(\theta_b) e^{i\delta_D(k_b)} \{N_g \cos[(k_b R_0/2)\cos\theta_b]; -iN_u \sin[(k_b R_0/2)\cos\theta_b]\}, \quad (4a)$$

$$\hat{\Theta}_Q^{(\lambda_Q)}(\theta_b) \rightarrow P_2^{(\lambda_2)}(\theta_b) e^{i\delta_Q(k_b)} \{N_g \cos[(k_b R_0/2)\cos\theta_b]; -iN_u \sin[(k_b R_0/2)\cos\theta_b]\}, \quad (4b)$$

where $\delta_D(k_b)$ and $\delta_Q(k_b)$ are the atomic phase shifts for $1s \rightarrow kp, kd$ ionization, respectively, k_b is the *body-frame* linear momentum of the photoelectron, the $N_{g/u}$ are normalization factors, and R_0 is the equilibrium bond distance. The diffractionlike $\cos[(k_b R_0/2)\cos\theta_b]$ and $-i\sin[(k_b R_0/2)\cos\theta_b]$ terms, corresponding to contributions from the $1\sigma_g$ and $1\sigma_u$ photoionization channels, respectively, are a consequence of off-center "atomic" electron ejection in the molecular geometry. Employing Eqs. (4) and extrapolating the expressions for $\delta(\hbar\omega)$ and $\gamma(\hbar\omega)$ to the atomic limit, where the molecule is treated as two isolated and noninteracting atoms, yields $\delta(\hbar\omega) \rightarrow 0$ and

$$\zeta(\hbar\omega) \rightarrow \gamma(\hbar\omega) \rightarrow 6(R_Q/R_D)k_p \cos[\delta_Q(k_b) - \delta_D(k_b)]. \quad (5)$$

These results are identical to the known atomic expressions, where R_Q/R_D, the ratio of quadrupole-to-dipole radial atomic transition moments, is expressed here in the momentum representation, rather than in the coordinate representation [6–8].

The atomic-limit predictions reported in Fig. 1 as a dash-dotted curve agree extremely well with previous calculations for atomic nitrogen [6]. Absent entirely is any evidence of the broad resonancelike feature in the measured data, nor is there any indication of the oscillatory behavior with increasing energy suggested by the measured values. Accordingly, the measured photon-energy variations reported in Fig. 1 evidently have a molecular origin, in spite of the largely atomiclike nature of the occupied $1s$ orbitals in nitrogen.

Calculations of dipolar and nondipolar molecular transition moments and angular-emission amplitudes for N_2 have been made in a single-channel static-exchange approximation in order to obtain a simple understanding of the molecular origins of the energy variations in the measured nondipole anisotropy parameter in Fig. 1. Such theoretical values are expected to be reliable at all photon energies depicted, except in the photoionization threshold region where target wave function distortions neglected in the static-exchange approximation can be significant. The result of this calculation (solid curve) can be understood as arising from the interplay of three contributing factors.

First, the photon-energy variations of the dipole transition moments, which are known from previous inner-shell studies [22–25], play a small but distinct role in the calculated results. Specifically, the $1\sigma_g \rightarrow k\sigma_u$ transition moment includes a prominent low-energy ($h\nu \approx 420$ eV) shape resonance [22–24], with a related weaker feature in the $1\sigma_u \rightarrow k\sigma_g$ moment arising from channel-coupling effects [25]; the other dipole transition moments $(1\sigma_{g/u} \rightarrow k\pi_{u/g})$ are unstructured and largely monotonic over the energy range of the broad feature appearing in Fig. 1. Accordingly, the resonancelike behavior in the data is not a direct consequence of the dipole terms and more particularly is not directly related to the well-known low-energy dipole shape resonance in molecular nitrogen. However, because the dipole cross section appears in Eq. (3), the dipole shape resonance in N_2, which depletes the continuum oscillator strength at higher photon energies, indirectly contributes to the increase in the nondipole feature of Fig. 1 with increasing photon energy.

Second, the angular emission amplitudes for the fully molecular treatment include diffractionlike terms similar to those in the high-photon-energy-limit expressions of Eqs. (4), but now including rescattering in the molecular field subsequent to off-center photoejection from the individual atomic sites. The bond-length dependence of these terms gives rise to pronounced photon-energy variations

in the associated normalization factors $N_{g/u}$, accounting largely for the shape of the calculated curve in Fig. 1. Similar bond-length-dependent oscillatory behaviors also arise in nondipole Raman scattering from diatomic molecules [26], and wave function normalization factors have been implicated previously in nondipole aspects of atomic photoionization [6]. It is important to recognize, however, that the diffractionlike terms of Eqs. (4) are strictly of molecular origin; they do not contribute to $\delta(\hbar\omega)$ and $\gamma(\hbar\omega)$ in the atomic limit [Eq. (5)] because the isotropy of the nondipole transition moments ensures that the cosine and sine factors combine as squares to eliminate the bond-length-dependent terms.

Third, the spatially compact nature of the atomic $1s$ orbitals ensures that nondipole $1\sigma_{g/u} \rightarrow k\sigma_{g/u}; k\pi_{g/u}; k\delta_{g/u}$ transition moments in N_2 extend to high photon energy, encompassing the spectral interval of the broad feature in the data of Fig. 1. To understand their energy variations in detail, it is helpful to note the nondipole transition moments are closely related to previously studied $1\pi_u \rightarrow k\sigma_g; k\pi_g; k\delta_g$ valence-shell dipole transition moments in N_2 [27,28] and to $1\pi_g$-shell moments in other small diatomic molecules [29]. This correspondence arises from the form of the nondipolar transition operators [20], which can be factored into products of dipole terms, one of which effectively gives the inner-shell $1\sigma_{g/u}$ orbitals $\pi_{u/g}$ character [i.e., $(x, y) \otimes 1\sigma_{g/u} \approx \pi_{u/g}$]. In this sense, the nondipole transition moments can be regarded as *dipole* transition moments connecting the continuum states with K-shell orbitals of effectively $\pi_{g/u}$ character. The spatially compact nature of these orbitals extends the energy variations of the resulting transition moments to significantly higher photon energy relative to those of the corresponding valence shell $1\pi_{g/u}$ dipole transition moments [25,27,28]. Moreover, the well-known predominance of the $1\pi_{g/u} \rightarrow k\delta_{u/g}$ components of π-shell photoionization cross sections in small diatomic molecules [27–29] indicates that the $1\sigma_{g/u} \rightarrow k\delta_{g/u}$ nondipole inner-shell transition moments in N_2 correspondingly provide the largest contributions, accounting for the magnitude of the broad maximum seen in Fig. 1.

The interplay among the three factors determining the energy variations of the nondipole photoionization anisotropy in N_2 has no evident counterpart in atoms and appears to be indicative of a universal nondipole behavior in molecular photoionization. There is also good reason to expect this molecular phenomenon will be present in condensed phases as well, indicating its potential relevance to techniques sensitive to electron angular-emission patterns from solids, such as x-ray standing-wave measurements [30], angle-resolved photoemission, and extended x-ray absorption fine structure, to suggest a few. Clearly, this unexpected discovery warrants further experimental and theoretical study.

Support provided in part by grants from the National Research Council, the U.S. Air Force Office of Scientific Research, the National Science Foundation, and the Department of Energy (DOE) is gratefully acknowledged. We thank Dr. Peter R. Taylor for his hospitality to P. W. L. at the San Diego Supercomputer Center during the course of the investigation. The authors thank the staff of ALS for their support. The ALS is funded by the DOE, Materials Sciences Division, Basic Energy Sciences, under Contract No. DE-AC03-76SF00098.

[1] H. A. Bethe and E. E. Salpeter, *Quantum Mechanics of One- and Two-Electron Atoms* (Springer-Verlag, Berlin, 1957).
[2] J. Berkowitz, *Photoabsorption, Photoionization, and Photoelectron Spectroscopy* (Academic, New York, 1979).
[3] C. N. Yang, Phys. Rev. **74**, 764 (1948).
[4] J. Cooper and R. N. Zare, J. Chem. Phys. **48**, 942 (1968).
[5] M. O. Krause, Phys. Rev. **177**, 151 (1969); F. Wuilleumier and M. O. Krause, Phys. Rev. A **10**, 242 (1974).
[6] A. Bechler and R. H. Pratt, Phys. Rev. A **39**, 1774 (1989); **42**, 6400 (1990).
[7] J. W. Cooper, Phys. Rev. A **42**, 6942 (1990); **47**, 1841 (1993).
[8] A. Derevianko, W. R. Johnson, and K. T. Cheng, At. Data Nucl. Data Tables **73**, 153 (1999).
[9] B. Krässig *et al.,* Phys. Rev. Lett. **75**, 4736 (1995).
[10] M. Jung *et al.,* Phys. Rev. A **54**, 2127 (1996).
[11] O. Hemmers *et al.,* J. Phys. B **30**, L727 (1997).
[12] N. L. S. Martin *et al.,* Phys. Rev. Lett. **81**, 1199 (1998).
[13] D. W. Lindle and O. Hemmers, J. Electron Spectrosc. Relat. Phenom. **100**, 297 (1999).
[14] A. Derevianko *et al.,* Phys. Rev. Lett. **84**, 2116 (2000).
[15] O. Hemmers *et al.,* Rev. Sci. Instrum. **69**, 3809 (1998).
[16] V. Dolmatov (private communication).
[17] B. Cleff and W. Mehlhorn, J. Phys. B **7**, 593 (1974).
[18] E. O. Berezkho and N. M. Kabachink, J. Phys. B **10**, 2467 (1977).
[19] N. M. Kabachink and I. P. Sazhina, J. Phys. B **29**, L515 (1996).
[20] P. W. Langhoff *et al.,* J. Electron Spectrosc. Relat. Phenom. **114–116**, 23 (2001).
[21] A. R. Edmonds, *Angular Momentum in Quantum Mechanics* (Princeton University Press, Princeton, NJ, 1957).
[22] J. L. Dehmer and D. Dill, J. Chem. Phys. **65**, 5327 (1976).
[23] T. N. Rescigno and P. W. Langhoff, Chem. Phys. Lett. **51**, 65 (1977).
[24] J. A. Sheehy *et al.,* J. Chem. Phys. **91**, 1796 (1989).
[25] N. A. Cherepkov *et al.,* Phys. Rev. Lett. **84**, 250 (2000).
[26] J. D. Mills *et al.,* Phys. Rev. Lett. **79**, 383 (1997).
[27] T. N. Rescigno *et al.,* J. Chem. Phys. **68**, 970 (1978).
[28] T. N. Rescigno *et al.,* Chem. Phys. Lett. **66**, 116 (1979).
[29] J. W. Gallagher *et al.,* J. Phys. Chem. Ref. Data **17**, 9 (1988).
[30] C. J. Fisher *et al.,* J. Phys. Condens. Matter **10**, L623 (1998).